Journal of Solid State Chemistry 182 (2009) 451–456

Contents lists available at ScienceDirect

Journal of Solid State Chemistry

journal homepage: www.elsevier.com/locate/jssc

Silver transfer in proustite Ag_3AsS_3 at high temperatures: Conductivity and single-crystal X-ray studies

Anna Gągor [a,*], Antoni Pawłowski [b], Adam Pietraszko [a]

[a] W. Trzebiatowski Institute of Low Temperature and Structure Research PAS, P.O. Box 1410, 50-950 Wrocław, Poland
[b] Institute of Molecular Physics PAS, Mariana Smoluchowskiego 17, 60-179 Poznań, Poland

ARTICLE INFO

Article history:
Received 13 August 2008
Received in revised form
3 November 2008
Accepted 9 November 2008
Available online 18 November 2008

Keywords:
Proustite
Ionic conductors
Impedance spectroscopy
X-ray diffraction

ABSTRACT

Single crystals of proustite Ag_3AsS_3 have been characterised by impedance spectroscopy and single-crystal X-ray diffraction in the temperature ranges of 295–543 and 295–695 K, respectively. An analysis of the one-particle potential of silver atoms shows that in the whole measuring temperature range defects in the silver substructure play a major role in the conduction mechanism. Furthermore, the silver transfer is equally probable within silver chains and spirals, as well as between chains and spirals. The trigonal *R3c* room temperature phase does not change until the decomposition of the crystal. The electric anomaly of the first-order character which appears near 502 K is related to an increase in the electronic component of the total conductivity resulting from Ag_2S deposition at the sample surface.

1. Introduction

A large number of studies on the structure and physical properties of proustite have been carried out since the discovery of many important technical applications of the compound. This photosensitive semiconductor is used in the field of acustoelectronics, non-linear optics and as a dielectric material, for example. The broad spectrum of possible practical uses has promoted detailed studies of the crystal structure of proustite, its phase transformations and its conductivity behaviour [1–5].

The room temperature structure of proustite is trigonal with *R3c* symmetry. Determined for the first time by Harker [6], this phenomenon was later confirmed by other authors [7,8]. Complex structural first- and second-order phase transitions were reported due to the change of the ordering degree of the silver substructure. In earlier papers, the second-order transition from the trigonal to the monoclinic *Pm* phase was reported at 210 K from Raman and Brillouin's scattering spectra study as well as dielectric and acoustic anomalies [9–11]. However, subsequent studies have failed to reveal any structural changes in the temperature range of 80–300 K [5,12]. According to Nelmes et al. [5] the trigonal phase is preserved down to ~61 K, where the transition to an incomensurately modulated phase occurs. Khasanov et al. [13] reported that additional diffraction peaks associated with modulation disappear below 28 K as a consequence of the first-order phase transition to the triclinic phase [11].

The ordering state of the silver substructure determines the transport properties of proustite. As the temperature rises, the conductivity changes from electronic at low temperatures to mixed electronic and ionic (Ag^+), with the ionic component dominating at ~230 K. At room temperature the conductivity exhibits an almost purely ionic character with a contribution of electronic conductivity of p type less than 1% [14–16]. The room temperature conductivity is $\sim 10^{-5}\,(\Omega\,\mathrm{cm})^{-1}$ and at 411 K, it reaches a value of $\sim 10^{-3}\,(\Omega\,\mathrm{cm})^{-1}$.

According to Yang and Taylor [1] the first-order phase transition at 420 K is related to the melting of the silver substructure and the transformation of the crystal to the superionic state. Despite the fact that on the basis of conductivity measurements the melting process of the silver substructure has been postulated, there is still a lack of data concerning the high temperature structure, possible phase transitions and the conduction mechanism at microscopic level.

Recently, Schonau and Redfern [17] reported a second-order phase transition at 305 K associated with a positive non-symmetrical break in the spontaneous strain of the unit cell resulting from the onset of thermally induced migration of Ag^+ ions. The substantial increase in conductivity observed at 420 K is attributed to the beginning of the melting process of the silver substructure. Next, the transition to the superionic phase with a molten silver substructure at ~540 K and the decomposition of

* Corresponding author. Fax: +48 71 343 10 29.
E-mail address: a.gagor@int.pan.wroc.pl (A. Gągor).

0022-4596/$ - see front matter © 2008 Elsevier Inc. All rights reserved.
doi:10.1016/j.jssc.2008.11.005

the crystal on further heating were reported. In the same paper, on the other hand, a thermal evolution of lattice parameters is reported at 600 K with no indication of a sample decomposition.

In the present work, the still controversial issue of the high temperature structure and the mechanism of silver migration is considered. A more precise picture of the processes which take place at high temperatures is crucial for analysing and understanding the results of electrical conductivity measurements. Here the results of single-crystal X-ray diffraction and impedance spectroscopy studies are presented which facilitates a report on the microscopic mechanism of silver conduction at high temperatures. The results point to the significance of decomposition processes and may contribute to the clarification of discrepancies in recent reports on the high temperature ionic conductivity and phase transitions in Ag_3AsS_3.

2. Experimental

2.1. Impedance spectroscopy study of electrical conductivity

The complex impedance of the proustite samples was measured in the temperature range of 295–543 K with a Hewlett-Packard 4192A LF Impedance Analyser at frequencies in 100–10 MHz range. The results were analysed in the complex $Z''(Z')$ plane.

Two samples oriented in [001] and [110] directions with average dimensions of $2\times2\times0.15$ mm were studied. The electrodes were prepared by covering the opposite faces of a sample with a silver paste (Demetron). Each complex impedance plot was obtained at a temperature stabilised to within 0.1 K and the sample resistance was found as the intercept of the plot with the real axis. Due to the sensitivity to light the samples were kept in darkness allowing for a one day recovery after exposure to light before the measurements.

2.2. Structure determination

A single-crystal X-ray study was performed on a Kuma KM4CCD diffractometer with graphite-monochromated Mo$K\alpha$ radiation. The CrysAlis. software version 1.170.32 (Oxford Diffraction) [18] was used for data processing and reciprocal space reconstruction. For all samples, an empirical absorption correction was applied using spherical harmonics, implemented in SCALE3 ABSPACK scaling algorithm. The room temperature structure model of proustite was applied [8] and refined by the full-matrix least squares method using a Jana2000 program package [19]. Diffraction data were collected in the range of 295–695 K. The details of the crystal structure investigations at 295, 415 and 695 K can be obtained from the Fachinformationszentrum Karlsruhe, 76344 Eggenstein-Leopoldshafen, Germany (fax: +497247808666; e-mail: crysdata@fiz.karlsruhe.de) using depositary numbers CSD 419203 (295 K), 419205 (415 K) and 419204 (695 K). The final coordinates with isotropic and anisotropic displacement parameters are presented in supplementary materials in Tables A.1 and A.2.

To account for the diffused electron density of silver, we extended the refinement on the anharmonic Gram–Chalier model of displacement parameters [20,21]. The displacement factors of silver atoms at all temperatures were refined in the third-order anharmonic approximation. The values of anharmonic terms (C_{ijk}) in the Gram–Chalier expansion are presented in supplementary materials in Table A.3. On the basis of silver joint probability density function (PDF) we analysed the change of the pseudopotential along possible diffusion paths versus temperature. In the case of resolved positions the potential difference between two symmetrically nonequivalent sites $\mathbf{x}_1$ and $\mathbf{x}_2$ is given by

$$V(\mathbf{x}_1)-V(\mathbf{x}_2)=-kT\ln[w_1PDF_1(\mathbf{x}_1)/w_2PDF_2(\mathbf{x}_2)] \quad (1)$$

where w_1 and w_2 are occupation factors [22].

Crystal data and experimental details are summarised in Table 1 together with the parameters of the structure refinement.

Powder diffraction data were collected on a stoe automatic powder diffraction system equipped with an image plate position sensitive detector, Cu$K\alpha_1$-radiation, Ge monochromator. The thermogravimetric analysis (TGA) and the differential thermal analysis (DTA) were performed on a Linseis L81 thermobalance. The measurements were performed in the temperature range of 295–850 K (heating rate = 5 K/1min) in the air.

Table 1
Crystal data, experimental details and structure refinement results for Ag_3AsS_3.

Formula	Ag_3AsS_3		
Temperature (K)	295	415	695
Radiation/wavelength (Å)		Mo$K\alpha$/0.71069	
Crystal system, space group		trigonal, R3c	
Z, Pearson code		6, hR20	
Lattice parameters a, c (Å)	10.814, 8.692	10.856, 8.724	10.913, 8.762
Volume (A^3)	880.19	890.5	903.7
Calculated density (g/cm^3)	5.60	5.53	5.45
$2\theta(^\circ)$ range for data collection	59.01	88.08	56.37
No. of ref. collected/unique	3233/515	4163/540	2796/468
R_{int}	0.047	0.031	0.033
Data/parameters	515/25	540/33	468/23
S_{all}	0.97	1.12	1.08
R_1, wR_2 ($I>3\sigma(I)$)	0.022, 0.028	0.019, 0.029	0.025, 0.030
R_1, wR_2 (all data)	0.028, 0.031	0.020, 0.030	0.038, 0.032
Extinction parameter	0.060(6)	0.066(5)	0.081(9)

3. Results and discussion

3.1. Structure description

The room temperature crystal structure of proustite was described for the first time in 1936 by Harker [6]. Since then, the structure has been revised several times [7,8]. Our study confirmed that the room temperature structure adopts a noncentrosymmetric space group $R3c$ (no. 161) with lattice parameters given in Table 1. The view of the proustite hexagonal unit cell structure is presented in Fig. 1.

The arsenic and sulfur atoms form covalently bonded AsS_3 pyramids aligned along the polar three-fold c axis. Alternate pyramids are related to each other through a c-glide plane. Silver atoms are distributed between the pyramids and link the AsS_3 complexes via ionic S–Ag–S′ links which form two sets of three-sided helices (right- and left-handed) parallel to the c axis. The silver substructure can also be regarded as three types of non-intersecting silver chains within the structure. With a temperature increase, the crystal symmetry does not change. Even at 695 K, the structure refinement in the $R3c$ space group gives highly satisfactory results. Table 2 presents selected distances and angles in the Ag_3AsS_3 crystal at 295, 415 and 695 K.

Before proceeding, note the structure in the temperature range of 295–695 K (within which the measurements were performed); Ref. [17] reports that the crystal decomposes at ~540 K. However, the results for single-crystal X-ray diffraction of Ag_3AsS_3 did not reveal any significant changes above 540 K. While it is true that some noticeable Debay–Scherrer rings appeared above 570 K, they did not influence the structure determination. Moreover, even at 695 K the sample X-ray showed good quality, despite the fact that a metallic tint appeared on its surface. The rotating crystal images

for the sample annealed for ~10 h at 570 K and then cooled to the room temperature, as well as at 695 K, are presented in Fig. 2.

To account for the effects mentioned above (i.e., the decomposition of the sample above 540 K and no significant structure change up to 695 K) we performed DTA and thermogravimetry (TG) measurements. The results are presented in Fig. 3. TG data indicate a significant (~18%) loss of mass of the sample in the range of 600–690 K. Two maxima which appear in the DTA diagram at 660 and 700 K point to two exothermic reactions accompanying the decomposition. To examine the reaction products, the X-ray diagram of the annealed powder sample (700 K, 1 h) was prepared, revealing that the whole sample decomposed to Ag_2S and some arsenic compounds which must have evapourated from the surface (probably as Ag_2S_3) since no As compounds were found in the powder diagram (see Fig. 4). Annealing of the powder sample at higher temperature (850 K) led to creation of metallic silver and Ag_2SO_4, see Fig. A.1.

The results of our single-crystal X-ray measurements indicate that the structure of proustite does not change up to 695 K and, therefore, seem to be inconsistent with the changes observed in DTA, TG and X-ray powder diagrams. A possible explanation is a much slower decomposition rate of a single crystal compared with a powder sample. The Ag_2S thin film which is created at the sample surface (seen as a metallic tint) suppresses further decomposition. The powder X-ray diagram of a remains of a single crystal annealed at 700 K for 4 h shows that the sample is still Ag_3AsS_3 with only a trace of Ag_2S (see Fig. 5).

Regarding the structure, no symmetry change up to 695 K was observed. Our structure analysis shows that silver ions do not tend to occupy any additional preferred lattice sites within the whole measuring temperature range. However, as the temperature rises, the values of the U_{11}, C_{111} and C_{133} atomic displacement

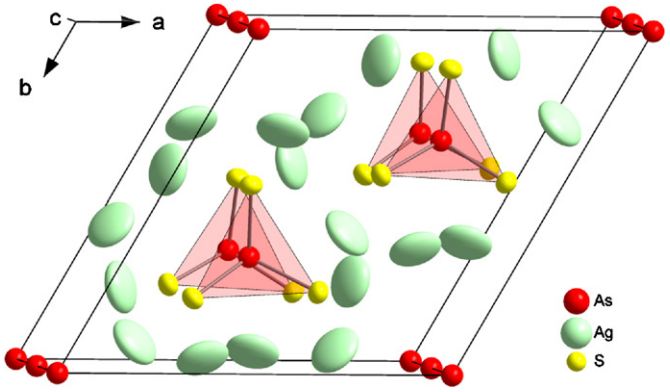

Fig. 1. The view of the proustite hexagonal unit cell structure, $T = 295$ K.

Table 2
Selected distances and angles in Ag_3AsS_3 at: $T = 295$, 415 and 695 K.

	295 K	415 K	695 K
Spirals Ag–S			
Ag–S	2.446(3)	2.457(3)	2.465(2)
Ag–S′	2.434(3)	2.436(2)	2.438(2)
Ag–S–Ag′	83.51(11)	84.22(7)	85.46(6)
S–Ag–S′	162.00(12)	161.22(7)	160.22(8)
Pyramids AsS_3			
As–S	2.2665(7)	2.270(2)	2.465(2)
S–S	3.452(2)	3.462(1)	3.473(1)
S–As–S	99.18(3)	99.39(8)	99.73(5)
Chains Ag AsS_3			
Ag–Ag	3.482(4)	3.496(3)	3.512(3)
Ag–Ag′–Ag″	162.46(9)	162.35(7)	162.70(7)

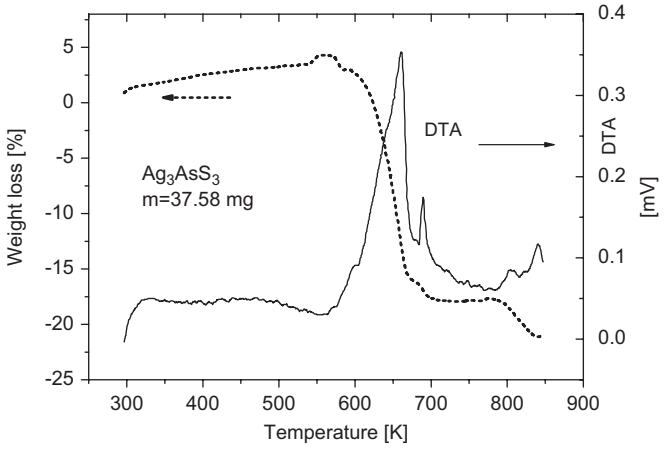

Fig. 3. DTA and TG.

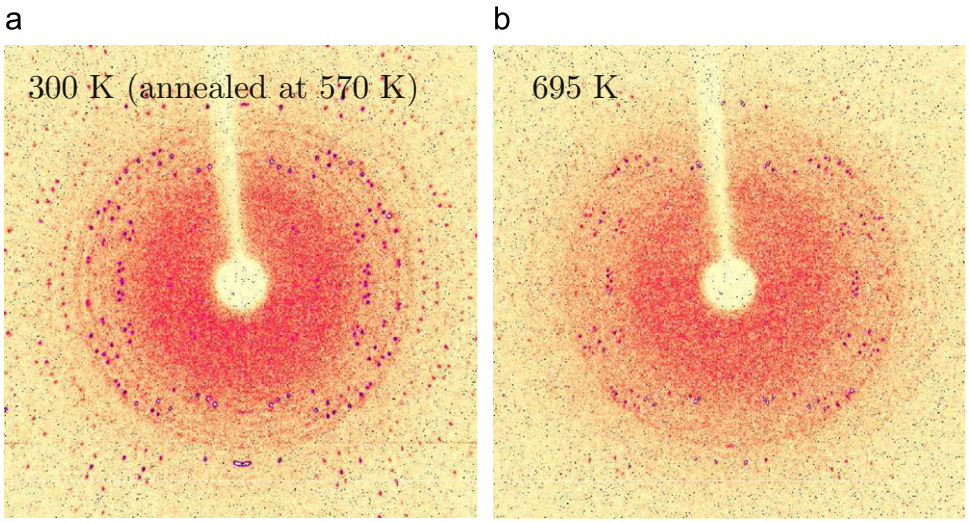

Fig. 2. The diffraction picture of the sample annealed (a) about 10 h at 570 K and then cooled to 300 K and (b) at 695 K.

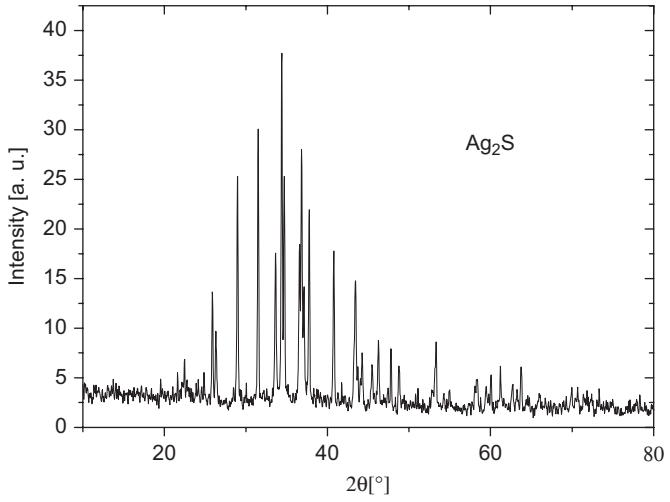

Fig. 4. Powder diagram, $T = 295$ K. The Ag_3AsS_3 powder annealed at 700 K for 1 h and then cooled to room temperature.

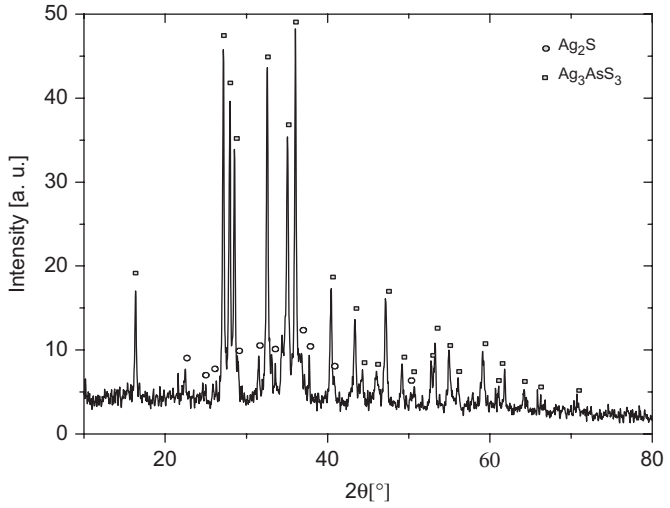

Fig. 5. Powder diagram, $T = 295$ K. The Ag_3AsS_3 single crystal annealed at 700 K for 4 h then cooled to room temperature and ground to powder.

parameters increase significantly (see Fig. 7). As a consequence, the PDF of silver smears toward a position *X* shown in Fig. 6. Even then, no significant superposition of the PDF of silver atoms is observed. The *X* position is similar to an additional lattice site found for Ag^+ ions after a possible symmetry increase at a high temperature [4]. In our study, no symmetry change up to 695 K was observed. Fig. 8 presents the joint PDF of silver atoms at 415 and 695 K. Diagrams have been prepared to consider all neighbouring silver positions. Ag1 and Ag2 positions belong to the same silver chain whereas Ag3 and Ag1 reside in one Ag–S–Ag spiral. The *X* position is set in the centre of the Ag1Ag2Ag3 triangle. The possible connections between the silver positions as well as the *X* position are presented in Fig. 6.

The joint PDF gives a unique value for the potential in the regions where single PDFs overlap. Thus, we have calculated the potential barrier along two possible diffusion paths (Ag1–Ag2–Ag3–Ag1 and Ag1–*X*–Ag2–*X*–Ag3–*X*–Ag1), exhausting the possible migration ways of silver. The potential within the first path is presented in Fig. 9(a). The lowest barrier of 0.47 eV is observed within the silver chain between Ag1 and Ag2 positions. The energy barrier of 0.53 eV between the silver chain and the spiral

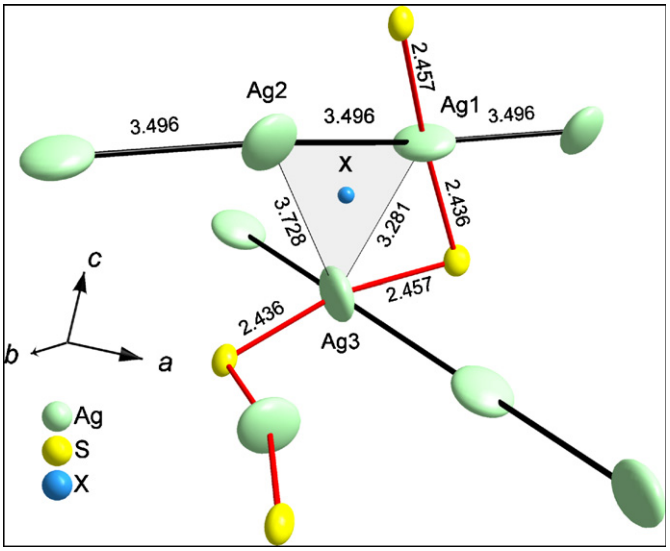

Fig. 6. Chains of silver and spirals S–Ag–S′, $T = 415$ K.

(Ag2–Ag3) is slightly higher whereas the silver migrations within one spiral (Ag1–Ag3) are largely suppressed by the potential barrier of 0.88 eV. In proustite, the distance between Ag1 and Ag3 is the shortest, with a value of 3.271 Å at room temperature.

Regarding the second conduction path (Ag1–*X*–Ag2–*X*–Ag3–*X*–Ag1), the potential barrier between Ag1 and A3 decreases drastically to 0.51 eV at room temperature. Almost the same energy barrier value was obtained between all silver positions, suggesting that not only is the silver transfer within the chains and between the chains and the spirals equally probable, but silver migrations within spirals are also possible.

Fig. 9 shows that the one-particle potential in proustite changes very little with temperature, indicating that even at high temperatures the structure of proustite is ordered, since the potential in ordered crystals is independent of temperature (apart from small effects due to the thermal expansion) [22]. The lack of the changes in one-particle potential with temperature indicates that defects in the silver substructure play a major role in the conduction mechanism. The melting of silver substructure is not observed, even above 500 K. Admittedly, the occupancy of silver positions decreases with temperature by 1% at 415 K and 3% at 695 K, see Table A.1, but they can be still regarded as the same within 3σ values.

3.2. Electrical conductivity

The temperature dependence of the total electric conductivity of Ag_3AsS_3 containing both the ionic and electron contribution was measured for two samples oriented in [001] and [110] directions, and the results are presented in Fig. 10. Conductivity in [110] direction is slightly higher than conductivity along [001], indicating an "easier" migration pathway in the (a,b) plane. However, the structure study data show the migrations of silver are equally probable in all directions. Taking into account that the conductivity difference between the samples is small and changes very little in the whole temperature range, a systematic measuring error is probably responsible for the conductivity difference.

In order to determine the activation energy of the cation mobility, the temperature dependent conductivity values were fitted to the Arrhenius formula

$$\sigma(T) = \sigma_0 e^{-\Delta E/kT} \quad (2)$$

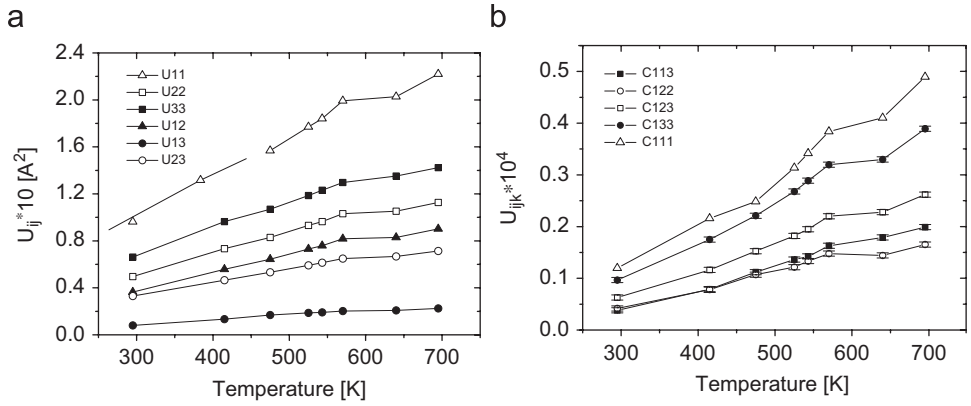

Fig. 7. Thermal evolution of silver anisotropic displacement parameters in Ag_3AsS_3 crystal (a) harmonic and (b) anharmonic parameters.

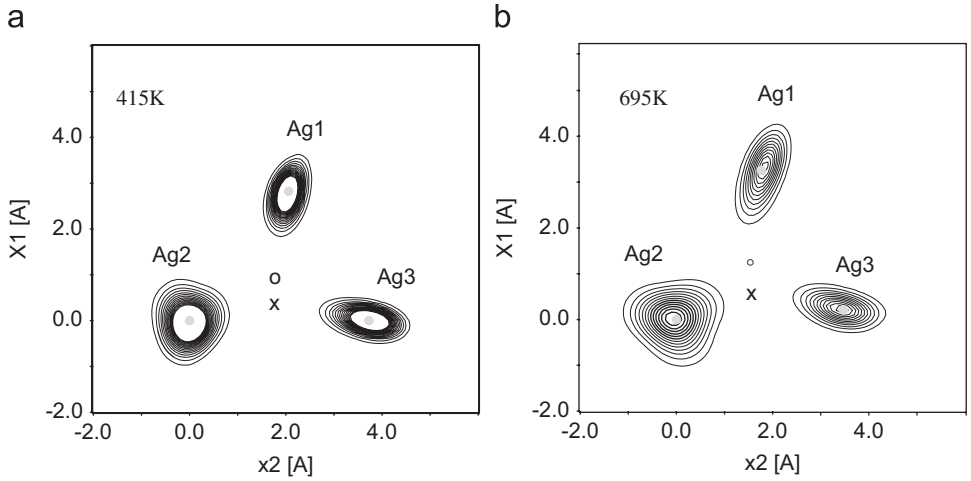

Fig. 8. Joint probability density function map of silver atoms (a) $T = 415$ K and (b) $T = 695$ K; section passing through Ag1, Ag2 and Ag3 positions marked in the picture.

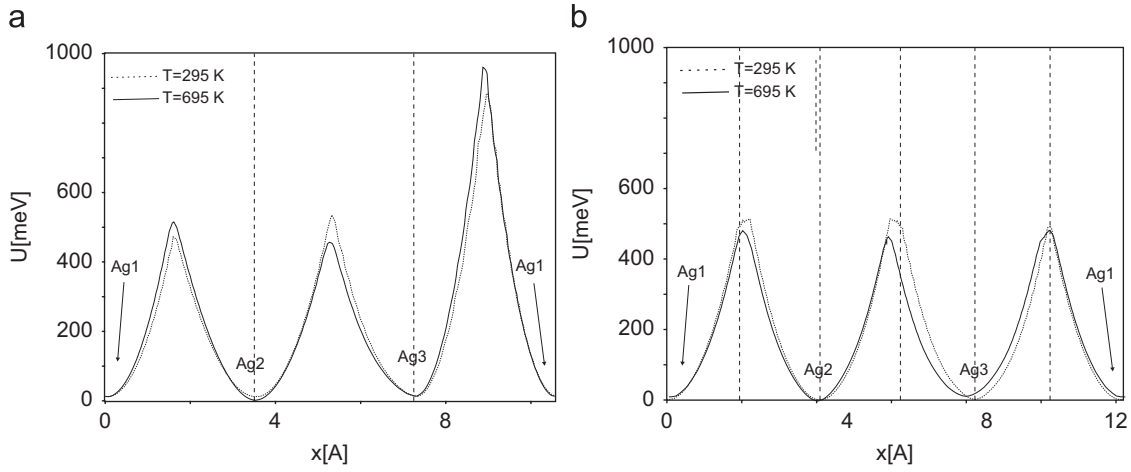

Fig. 9. One-particle potential along the (a) Ag1–Ag2–Ag3–Ag1 and (b) Ag1–*X*–Ag2–*X*–Ag3–*X*–Ag1.

where σ_0 and ΔE denote the pre-exponential factor and the activation energy, respectively, and k is the Boltzmann constant.

The superionic phase transition reportedly occurring at 420 K [1] was undetected both in the magnitude of ionic conductivity and in the activation energy value, and the high temperature phase transition revealed at 502 K does not coincide with any of the phase transitions reported for this compound to date.

The results of our study point to two possible sources of the total conductivity rise in Ag_3AsS_3 with a temperature increase: (i) thermally activated hopping motion of Ag^+ ions and (ii) the formation of an Ag_2S deposit on the surface of a sample. As it was pointed out in [14–16] process (i) is already started far below 502 K. Also process (ii) probably begins most likely below this temperature. Ag_2S exhibits a mixed ionic–electronic conductivity.

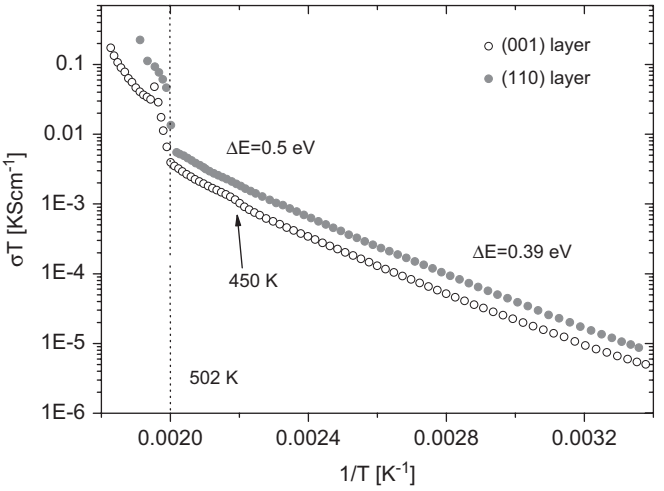

Fig. 10. Temperature dependence of electric conductivity of proustite single crystal along [001] and [110] direction.

Above the phase transition from β to α form at $T = 450$ K, its conductivity is electronic with an insignificant contribution of Ag^+ transport, depending very little on temperature. Hence, we interpret the behaviour of the total electric conductivity of Ag_3AsS_3 as follows: below 502 K the conductivity results from Ag^+ diffusion, and its slow increase in a large temperature range is due to process (i). At the same time, process (ii) slowly proceeds, and at 502 K a percolation threshold of the Ag_2S layer on the surface is reached, resulting in a stepwise increase in the total conductivity which becomes mainly electronic.

Below 502 K, the conductivity of the proustite obtained in our study is lower than the conductivity reported previously [23]. A fit of the data to the Arrhenius law yields an activation energy of 0.39 eV below 450 K compared with 0.28 eV obtained earlier [1]. Above 450 K the fit provides the activation energy $E = 0.50$ eV which does not differ in the limit of error from $E = 0.51$ eV previously reported for this temperature range [24]. Fig. 10 shows that the value of conductivity changes from $\sigma = 5.1 * 10^{-6}\,S\,cm^{-1}$ at $T = 297$ K to $\sigma = 4.0 * 10^{-3}\,S\,cm^{-1}$ at $T = 501$ K and after the jump at 502 K it rises to $\sigma = 0.1\,S\,cm^{-1}$ at $T = 543$ K.

The maximum potential barrier in proustite of 0.5 eV (calculated on the basis of the joint PDFs via additional X position) perfectly agrees with the experimental value of the activation energy of conductivity.

4. Summary

Ag_3AsS_3 has been characterised by impedance spectroscopy and single-crystal X-ray diffraction in the temperature ranges of 295–543 and 295–695 K, respectively. Structural analysis indicates that the trigonal $R3c$ room temperature phase does not change until the decomposition of the crystal without any indications of structural phase transitions. The analysis of the one-particle potential of silver ions shows that in the entire measured temperature range, the major role in the conduction mechanism in the bulk is controlled by defects in the silver substructure. Furthermore, the silver transfer is equally probable within silver chains, spirals, and between chains and spirals. The energy barrier obtained from the joint probability density function analysis perfectly matches the activation energy of the conductivity of measured samples.

The high temperature analysis of the total conductivity of proustite is not straightforward. Above 500 K it is necessary to consider the influence of decomposition processes at the surface on measured physical properties. Hence, the electrical conductivity anomaly which appears at 502 K is probably related to the increase in the electronic contribution to the total conductivity as a result of Ag_2S deposition at the surface.

Acknowledgment

The authors thank Mrs. Ewa Bukowska from the INTiBS PAN, Wrocaw, Poland, for the DTA and TG measurements.

Appendix A. Supplementary data

Supplementary data associated with this article can be found in the online version at doi:10.1016/j.jssc.2008.11.005.

References

[1] S.R. Yang, K.N.R. Taylor, J. Appl. Phys. 67 (1990) 3387.
[2] S.R. Yang, K.N.R. Taylor, Phase Transitions 36 (1991) 233.
[3] S.R. Yang, K.N.R. Taylor, J. Appl. Phys. 69 (1990) 420.
[4] T.D. Kruszelnicka, Solid State Phys. 22 (1980) 1046.
[5] R.J. Nelmes, C.J. Howard, T.W. Ryan, W.I.F. David, A.J. Schultz, P.C. Leung, J. Phys. C 17 (1984) L861.
[6] D. Harker, J. Chem. Phys. 42 (1936) 381.
[7] P. Engel, W. Nowacki, Neues Jahrb. Mineral. Monatsch. 8 (1966) 181.
[8] S. Allen, Phase Transitions 6 (1985) 1.
[9] G.A. Smolenskii, I.G. Sinii, E.G. Kuzminov, A.A. Ggodovikov, Sov. Phys. Solid State 21 (1979) 1343.
[10] L.A. Kot, S.D. Prokhorova, Y.M. Sandler, I.G. Sinii, I.N. Flerov, Sov. Phys. Solid State 25 (1983) 884.
[11] A.D. Balyaev, V. Machulin, D.F. Baisa, A.V. Bondar, A.Y. Gordon, Sov. Phys. Solid State 19 (1977) 2161.
[12] P.J.S. Ewen, W. Taylor, G.L. Paul, J. Phys. C 16 (1983) 6475.
[13] S.S. Khasanov, V.S. Shethtman, I.M. Shmytko, Sov. Phys. Solid State 26 (1984) 572.
[14] V.B. Zlokazov, L.Y. Kobelev, S.V. Karpachev, Sov. Phys. Dokl. 26 (1981) 684.
[15] P.H. Davies, C.T. Elliott, K.F. Hulme, J. Phys. D 2 (1969) 165.
[16] V.I. Bredikhim, V.I. Genkin, L.V. Sustov, Sov. Phys. Solid State 18 (1976) 833.
[17] K.A. Schonau, S.A.T. Redfern, J. Appl. Phys. 92 (2002) 7415.
[18] M. Mayer, CrysAlis Programs for Data Collection and Reduction, Version 1.170.32, Oxford Diffraction Ltd., 2007.
[19] V. Petricek, M. Dusek, L. Palatinus, JANA2000, Institute of Physics, Praga, Czech Republic, 2000.
[20] P. Coppens, X-ray Charge Densities and Chemical Bonding, Oxford University Press, Oxford, 1997.
[21] W.F. Kuhs, Acta Crystallogr. A39 (1983) 148.
[22] R. Bachmann, H. Schulz, Acta Crystallogr. A40 (1984) 668.
[23] J. Warner, J. Phys. D 1 (1968) 1968.
[24] V.B. Zlokazov, L.Y. Kobelev, S.V. Karpachev, Sov. Phys. Dokl. 28 (1981) 176.